

Method for generating a photonic NOON state with quantum dots in coupled nanocavitiesKenji Kamide,^{1,*} Yasutomo Ota,¹ Satoshi Iwamoto,^{1,2} and Yasuhiko Arakawa^{1,2}¹*Institute for Nano Quantum Information Electronics (NanoQuine), University of Tokyo, Tokyo 153-8505, Japan*²*Institute of Industrial Science, University of Tokyo, Tokyo 153-8505, Japan*

(Received 17 February 2017; published 27 July 2017; publisher error corrected 2 August 2017)

We propose a method to generate path-entangled NOON-state photons from quantum dots and coupled nanocavities. In the systems we considered, cavity mode frequencies are tuned close to the biexciton two-photon resonance. Under appropriate conditions, the system can have the target NOON state in the energy eigenstate, as a consequence of destructive quantum interference. The NOON state can be generated by a resonant laser excitation. This method, first introduced for a two-photon NOON state ($N = 2$), can be extended toward a higher NOON state ($N > 2$) based on our recipe, which is applied to the case of $N = 4$ as an example.

DOI: [10.1103/PhysRevA.96.013853](https://doi.org/10.1103/PhysRevA.96.013853)**I. INTRODUCTION**

A fundamental question to the coherence of laser light [1] developed quantum optics [2]—a research field on quantum light—which has explored functionality and application of light inaccessible by classical light. Single photons are indispensable for quantum information processing [3–5] and quantum communication [6–9]. A multiphoton source allows for multiphoton imaging for medical purpose, making possible imaging deep inside the human brain with both increased penetration length and reduced damaging tissue [10,11]. Recent observation showing sensitivity of biological photoreceptors to photon statistics [12,13] indicates potential impact of using quantum light in research of biology, as recognized in terms of quantum biology [14]. The situation in turn is accelerating theoretical studies for a new quantum light source [15] and new applications [16].

An attractive application that takes advantage of quantum light is the one using NOON state. Photonic NOON state [17] is a kind of entangled Fock (number) state of two orthogonal modes, defined by

$$|\text{NOON}\rangle \equiv \frac{|N,0\rangle + |0,N\rangle}{\sqrt{2}} = \frac{(a_1^\dagger)^N + (a_2^\dagger)^N}{\sqrt{2 \times (n!)}} |\text{vac}\rangle, \quad (1)$$

where a_1^\dagger and a_2^\dagger are the creation operators of modes 1 and 2 and $|\text{vac}\rangle$ is the vacuum state. In particular, path-entangled NOON state, in which the two modes are located in different optical paths, can be used for phase-supersensitive quantum lithography [18] and quantum metrology [19,20], as shown by the entanglement-enhanced microscope [21]. Using NOON-state photon source in interferometry, the phase error can be reduced to the so-called Heisenberg limit that cannot be achieved by classical laser light [22,23]. Since the phase sensitivity increases with the photon number, such application requires generation of NOON states with large N . However, realization of an efficient source of NOON state with large N has been a challenging issue, especially in an optical regime (in contrast to microwave regime [24,25]).

A popular approach to generate photonic NOON state is based on the use of photons generated from spontaneous parametric down conversion (SPDC) processes in nonlinear

χ_2 crystal [26], linear optical elements, and postselection [23,27–29]. However, the approach results in the low generation rate and the generation occurs in a nondeterministic way. This is essentially because the SPDC photon source is strongly affected by classical noise from the pump lasers [2].

Another approach is to use true quantum light source based on quantum emitters with strong optical nonlinearity. Quantum dots (QDs) are ideal solid-state quantum emitters [30], whose emission rate can be increased further by embedding them inside photonic nanocavities [31–35]. The efficient generation method of polarization entangled two-photon NOON state ($N = 2$) was proposed theoretically by using two polarization modes of nanocavity [36,37]. On the other hand, a method using QD-nanocavity systems for higher NOON states with $N > 2$ has not been reported.

In this paper we propose a method to generate path-entangled NOON states with QDs in coupled nanocavities [38–45], called photonic molecules [38]. In our method, photons emitted from each of the two cavities, which can be guided into two separated optical paths, can form the path-entangled NOON state. A key idea in this method is utilizing the quantum interference between multiple quantum paths, being similar to the concept used for pure single-photon generation in coupled-cavity systems with weak optical nonlinearity [46,47]. This method has some advantages over the past approaches; the high-rate and on-demand emission of two-photon NOON state becomes possible. Moreover, extension toward higher-NOON-state generation is possible for the general case of $N(>2)$.

This paper is organized as follows. In Sec. II, we first show our method for 2002-state generator in a system with a QD in coupled nanocavities. Then, we evaluate performance of the 2002-state generator by simulating purity and available generation rate. In Sec. III, we generalize the method to $N > 2$, where a numerical simulation for 4004-state generator is also presented as an example. This paper is summarized and the conclusion is made in Sec. IV, where we also mention the comparison with the existing method on 2002-state generator [36,37] and future issues.

II. GENERATION METHOD OF 2002 STATE

Here we show how to generate two-photon NOON states in QD-coupled cavity systems. The generation method is explained in several steps. In the following four subsections,

*kamide@iis.u-tokyo.ac.jp

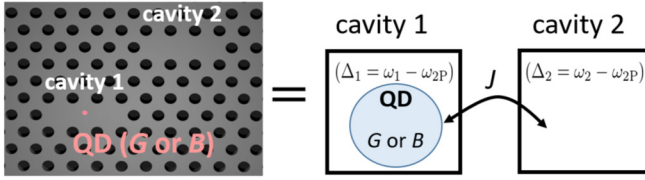


FIG. 1. Schematic of the QD-coupled nanocavity system for the two-photon NOON state (right), which can be realized in a PhC platform (left).

we explain our method by showing how to prepare 2002-state generating state “2002-GES” (named later) as an energy eigenstate of the system, how to excite 2002-GES, decay dynamics of the excited 2002-GES, and the available detection rate of the 2002-state photons emitted out from the cavities, in Secs. II A, II B, II C, and II D, respectively. Through the discussion, we show the essence of this scheme, which can be generalized to the case of $N > 2$ in Sec. III.

A. Preparation of 2002-GES in QD-coupled-cavity systems

The system we consider is composed of two nanocavities, cavity 1 and cavity 2, coupling through tunneling (tunneling rate J), and a QD in cavity 1 (coupling constant g), as shown in Fig. 1. This system can be realized in nanocavities, using micropillars [38–40], microdisks [41], and photonic crystals (PhCs) [42–45]. Cavity resonance frequencies (ω_1 and ω_2 for cavity 1 and cavity 2, respectively) are tuned close to the QD-biexciton two-photon resonance, $\Delta_{1(2)} \equiv \omega_{1(2)} - \omega_{2P} \sim 0$ [48], where $\omega_{2P} \sim (2\omega_X - \chi)/2$, and $\hbar\omega_X$ and $\hbar\chi$ are single-exciton energy and biexciton-binding energy in the QD (we set $\hbar = 1$ hereafter). In this case, by truncating the irrelevant single-exciton states, the effective Hamiltonian is approximated by [49]

$$H_{\text{eff}} = \sum_{j=1,2} \Delta_j a_j^\dagger a_j + J(a_1^\dagger a_2 + a_2^\dagger a_1) + g_{2P}(a_1^2 |B\rangle\langle G| + |G\rangle\langle B|(a_1^\dagger)^2), \quad (2)$$

where $g_{2P} = 4g^2/\chi$, a_j is an annihilation operator of photons in cavity $j (= 1, 2)$, and $|G\rangle$ and $|B\rangle$ represent the vacuum and biexciton states of the QD. This approximation can be used if cavities are tuned to the biexciton two-photon resonance, as far as $g \ll \chi/2$, whose validity is confirmed theoretically [49] and experimentally [48].

Typical value of the coupling constant is $g \sim 100 \mu\text{eV}$ [50] in a PhC platform, and the biexciton binding energy χ ranges between sub to few meV [48] (which can be electrically controllable [51]). For $g = 100 \mu\text{eV}$ and $\chi = 0.8 \text{ meV}$, the two-photon coupling constant g_{2P} is estimated to be $50 \mu\text{eV}$. Strong two-photon nonlinearity is observable if the cavity loss rate κ is smaller than g_{2P} . g_{2P} and $1/g_{2P}$ define characteristic energy and time scale for this system. The cavity detuning Δ_j can be controlled in some ways, e.g., by temperature tuning technique [32,52] and by xenon gas deposition technique [53]. Tunneling parameter J depends on the distance between cavities, meV order for direct coupling [42], and tens of μeV for waveguide mediated coupling [43]. Especially for the latter

case, J is electrically controllable [54] with high precision in μeV range, using an extra control cavity [55].

Our strategy for generating a pure 2002 state is to find conditions for three parameters, Δ_1/g_{2P} , Δ_2/g_{2P} , and J/g_{2P} , so that the two-photon NOON state can be included in the eigenstate of H_{eff} in Eq. (2). If we could find the condition, the eigenstate, which emits 2002-state photons out from the cavities, can be exclusively excited in the system by resonant pumping in the presence of the strong two-photon nonlinearity ($\kappa < g_{2P}$). In this sense, we shall call such an eigenstate “2002-state generating eigenstate (2002-GES).”

Noticing that H_{eff} commutes with the total excitation number operator, $[N_{\text{tot}}, H_{\text{eff}}] = 0$ with $N_{\text{tot}} = 2|B\rangle\langle B| + a_1^\dagger a_1 + a_2^\dagger a_2$, we focus on the eigenequation in the Hilbert subspace of $N_{\text{tot}} = 2$, $H_{2P}|E\rangle = E|E\rangle$, where

$$H_{2P} = \begin{pmatrix} 0 & \sqrt{2}g_{2P} & 0 & 0 \\ \sqrt{2}g_{2P} & 2\Delta_1 & \sqrt{2}J & 0 \\ 0 & \sqrt{2}J & \Delta_1 + \Delta_2 & \sqrt{2}J \\ 0 & 0 & \sqrt{2}J & 2\Delta_2 \end{pmatrix}, \quad (3)$$

and $|E\rangle = (A_B, A_{20}, A_{11}, A_{02}) = A_B|B, 00\rangle + A_{20}|G, 20\rangle + A_{11}|G, 11\rangle + A_{02}|G, 02\rangle$. A state vector, $|i, n_1 n_2\rangle$, represents QD state $i (= B \text{ or } G)$ with n_1 and n_2 photons in cavity 1 and cavity 2, respectively. The 2002-GES which we want to prepare in the system is an eigenstate $|E\rangle$ with $|A_{20}| = |A_{02}|$ and

$$A_{11} = 0. \quad (4)$$

Under the requirement, Eq. (4), the third row of $H_{2P}|E\rangle = E|E\rangle$ gives $J(A_{20} + A_{02}) = EA_{11} = 0$. Therefore, $|A_{20}| = |A_{02}|$ is automatically fulfilled with Eq. (4) for any nonzero J . There are two solutions to the eigenequation under Eq. (4), which are labeled by $s (= \pm)$. For the detuning parameters satisfying

$$\Delta_2 = \frac{\Delta_1 + s\sqrt{\Delta_1^2 + 2g_{2P}^2}}{2}, \quad (5)$$

one of the four eigenstates of H_{2P} and the eigenenergy are given by

$$|E_s\rangle = \cos \varphi_s |B, 00\rangle + \sin \varphi_s \left(\frac{|G, 20\rangle - |G, 02\rangle}{\sqrt{2}} \right), \quad (6)$$

$$E_s = \Delta_1 + s\sqrt{\Delta_1^2 + 2g_{2P}^2}, \quad (7)$$

where $\varphi_s \equiv \arctan(E_s/g_{2P})$.

The condition and the solution can be interpreted as follows. The requirement on cavity tuning, Eq. (5) [plotted in Fig. 2(a)], arises in order to satisfy Eq. (4). The 2002-GES, $|E_s\rangle$, is a superposition state of a biexciton state, $|B, 00\rangle$, and photonic 2002 state, $\frac{|G, 20\rangle - |G, 02\rangle}{\sqrt{2}}$, with probability ratio $(\tan \varphi_s)^2$, while only the latter component contributes to photon emission through the cavity loss. It is remarkable that all the above conditions, eigenstates, and eigenenergies are independent of J . This originates from the fact that the requirement in Eq. (4) is fulfilled for any nonzero J as far as $A_{20} = -A_{02}$. The third

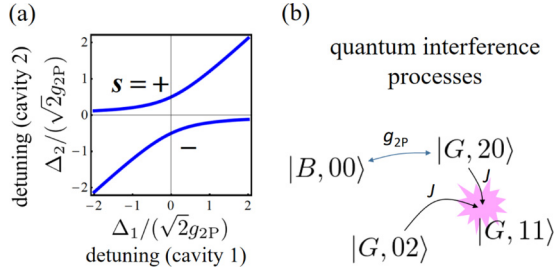


FIG. 2. (a) Required condition for the cavity detunings, Δ_1 and Δ_2 , so that the two-photon NOON state become one of the four energy eigenstates. (b) Quantum interference processes in the system described by Eq. (2). Arrows indicate the direction of coherent population flow at an initial time starting from the prepared 2002-GES ($|E\rangle$ with $A_{11} = 0$). In the figure, arrows connected to $|G, 11\rangle$ are unidirectional since the initial state does not contain $|G, 11\rangle$, hence with no outflow from it.

row of the Schrödinger equation $i \frac{d}{dt} |E\rangle = H_{2P} |E\rangle$,

$$i \frac{d}{dt} A_{11} = J(A_{20} + A_{02}), \quad (8)$$

shows that if $A_{20} = -A_{02}$ is satisfied, the quantum interference between two processes, $|G, 20\rangle \rightarrow |G, 11\rangle$ and $|G, 02\rangle \rightarrow |G, 11\rangle$, becomes fully destructive and the generation rate of the unwanted state $|G, 11\rangle$ vanishes irrespective of J [Fig. 2(b)].

While E_s does not depend on J , energies of the other three two-photon eigenstates do. Therefore, the 2002-GES can be excited exclusively by resonant laser pumping with a frequency $\omega_p - \omega_{2P} = E_s/2$, if J is selected properly to isolate it from others [as shown below in Fig. 5(a)] so that photon blockade effect [56,57] can work.

B. Excitation of 2002-GES in the system

The 2002-GES can be excited resonantly thanks to the strong optical nonlinearity. This can be confirmed by solving numerically the quantum master equation (QME) within Born-Markov approximation [58], taking into account the cavity decay processes. In the simulation, we have made several assumptions. To simplify discussion, we assumed that the energy dissipation is dominated by cavity loss, while the spontaneous emission of the QD excitons and biexcitons directly to free space can be negligible in a PhC platform, due to photonic band gap effect. In addition, we consider a case where the two cavities have the same loss rate κ . These assumptions do not change our main conclusion.

We start our analysis for cw excitation. In a frame rotating with the excitation laser frequency ω_p , the QME is given by

$$\frac{d}{dt} \rho = \mathcal{L} \rho = \frac{1}{i} [H'_{\text{eff}} + H_{\text{pump}}, \rho] + \mathcal{L}_{\text{loss}} \rho, \quad (9)$$

$$H'_{\text{eff}} \equiv H_{\text{eff}} - (\omega_p - \omega_{2P}) N_{\text{tot}}. \quad (10)$$

Here, $\mathcal{L}_{\text{loss}} (\equiv \kappa(\mathcal{L}_{a_1} + \mathcal{L}_{a_2}))$ represents the cavity loss and $H_{\text{pump}} (\equiv \Omega(a_2 + a_2^\dagger))$ describes cw pumping on cavity 2 with the Rabi field amplitude Ω (see also Appendix A). For a parameter set $(\kappa, J, \Delta_1, \Delta_2, \omega_p - \omega_{2P}, \Omega) = (0.1, 2, 1, -0.207, -0.207, 0.05) \times \sqrt{2}g_{2P}$ satisfying the condition,

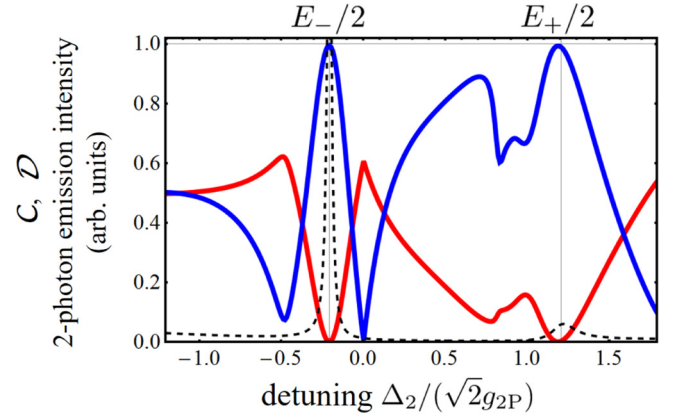


FIG. 3. Two-photon emission properties under weak cw pumping on cavity 2 are shown as a function of $\Delta_2 (= \omega_p - \omega_{2P})$: Concurrence \mathcal{C} (blue solid), trace distance \mathcal{D} (red solid), and normalized two-photon emission intensity (black dashed). Simulation is performed for parameters $(\kappa, J, \Delta_1, \Omega) = (0.1, 2, 1, 0.05) \times \sqrt{2}g_{2P}$.

Eq. (5) ($\Delta_2 = E_-/2$ for $s = -$), the cw laser excitation can generate the 2002-GES, which emits 2002-state photons. In general, laser excitation can result in multistate generation. However, as we shall see below, the multistate probability can be reduced thanks to the strong few-photon nonlinearity in the nanocavity systems. The quantum state of the emitted photons can be observed by the state tomography. In this case, the two-photon density matrix to be observed, ρ_{tomo} (defined in Appendix B), is found to be

$$\begin{pmatrix} 0.500 & -0.001 + 0.018i & -0.495 - 0.049i \\ -0.001 - 0.018i & 0.002 & -0.002 + 0.018i \\ -0.495 + 0.049i & -0.002 - 0.018i & 0.498 \end{pmatrix},$$

which is very close to those for pure 2002 states. The purity of the generated 2002 state is quantified by the trace distance from the pure 2002 state \mathcal{D} and concurrence \mathcal{C} ($\mathcal{D} = 0$ and $\mathcal{C} = 1$ correspond to an ideal case where pure 2002 state is generated: see Appendix B for the details). The above result gives small trace distance, $\mathcal{D} = 0.0007$, and high concurrence, $\mathcal{C} = 0.995$.

In Fig. 3, in order to see how effective the parameter tuning at the condition [Eq. (5)] is, we plotted the two-photon emission properties as a function of the cavity frequency Δ_2 . Here we consider weak cw pumping on cavity 2 (with the laser frequency $\omega_p = \Delta_2$). It is clear that the concurrence \mathcal{C} approaches unity and the trace distance \mathcal{D} approaches zero just at the two points, $\Delta_2 = E_-/2 \approx -0.207 \times \sqrt{2}g_{2P}$ and $\Delta_2 = E_+/2 \approx 1.207 \times \sqrt{2}g_{2P}$, which also locate at the peaks of two-photon emission intensity. This shows that the 2002-GES can be excited exclusively, hence the pure 2002-state photons can be generated, if the cavity frequencies are tuned at the condition. High contrast in the emission intensity at two peaks comes from the difference in the generated population and also in the decay rate (or emissivity) of the target states, $|E_s\rangle$, which depend also on the details of the energy level structure of intermediate one-photon states (see Appendix C).

Figure 4 shows the simulated concurrence \mathcal{C} as a function of cavity loss κ and the Rabi frequency Ω , for $(J, \Delta_1) = (2.0, 1.0) \times \sqrt{2}g_{2P}$ with which Eq. (5) is fulfilled. High value

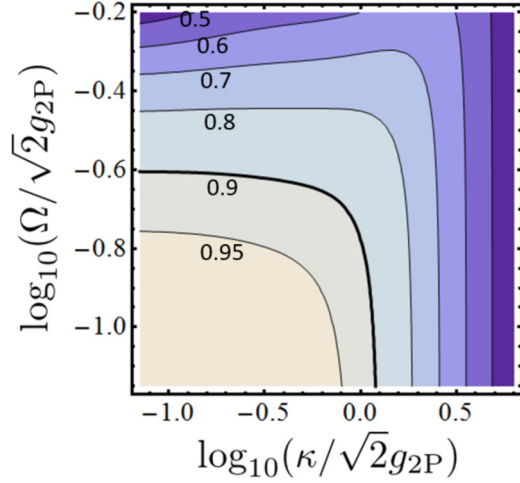


FIG. 4. Contour plot of the concurrence \mathcal{C} as a function of cavity loss κ and laser Rabi frequency Ω , for the case of cw resonant pumping on cavity 2 ($\Delta_2 = \omega_p - \omega_{2P} = E_-/2 = -0.207 \times \sqrt{2}g_{2P}$). Simulation is performed for parameters $(J, \Delta_1) = (2.0, 1.0) \times \sqrt{2}g_{2P}$.

of \mathcal{C} is observed for small κ and Ω ($\mathcal{C} > 0.9$ for $\kappa/\sqrt{2}g_{2P} < 1$ and $\Omega/\sqrt{2}g_{2P} < 0.25$). This can be understood as follows: the purity of the generated 2002-state photons becomes high for high- Q cavities because the 2002-GES can be spectrally isolated from other states and hence can be excited exclusively if the cavity linewidth κ is smaller than the level spacings of $O(J)$ and/or $O(g_{2P})$. However, even with high- Q cavity, the purity degrades with pumping strength due to state mixing of the higher-number Fock states in the case of $\Omega > O(J)$.

Alternatively, the 2002-GES can be excited in a deterministic way by using short Rabi pulse, whereas the cw excitation discussed above is a probabilistic way. Dynamics of the system during the pulsed generation is described by two-photon Rabi oscillation if one-photon excitation is negligible. This is possible with a proper choice of J . For example, for H'_{eff} , there exist two one-photon eigenstates,

$$|1P, +\rangle = \cos \phi |G, 10\rangle + \sin \phi |G, 01\rangle, \quad (11)$$

$$|1P, -\rangle = -\sin \phi |G, 10\rangle + \cos \phi |G, 01\rangle, \quad (12)$$

with $\phi = \arctan(\sqrt{1 + (\frac{\Delta_1 - \Delta_2}{2J})^2} - \frac{\Delta_1 - \Delta_2}{2J})$, whose eigenenergy is $E'_{1P, \pm} = E_{1P, \pm} - (\omega_p - \omega_{2P})$ with

$$E_{1P, \pm} = \frac{\Delta_1 + \Delta_2}{2} \pm \sqrt{\left(\frac{\Delta_1 - \Delta_2}{2}\right)^2 + J^2}. \quad (13)$$

As seen clearly, $E_{1P, \pm}$ depends on J , while the energy of the 2002-GES, E_s , does not. Therefore, if these one-photon states are detuned from the 2002-GES by tuning J , it is possible to excite the 2002-GES exclusively without generating one-photon states. Similarly, the 2002-GES can be detuned from the other two-photon eigenstates with proper choice of J . As an example, we plotted in Fig. 5(a) the eigenenergies of H'_{eff} in Eq. (10) sorted by the total number of excitations N_{tot} , for $(J, \Delta_1) = (5, 5) \times \sqrt{2}g_{2P}$ and $\Delta_2 = \omega_p - \omega_{2P} = E_-/2$. The resonance excitation from the ground state $|G, 00\rangle$ occurs to a state with eigenenergy of zero, whose candidate is only $|E_-\rangle$, the 2002-GES, for this parameter. [We note that generation of

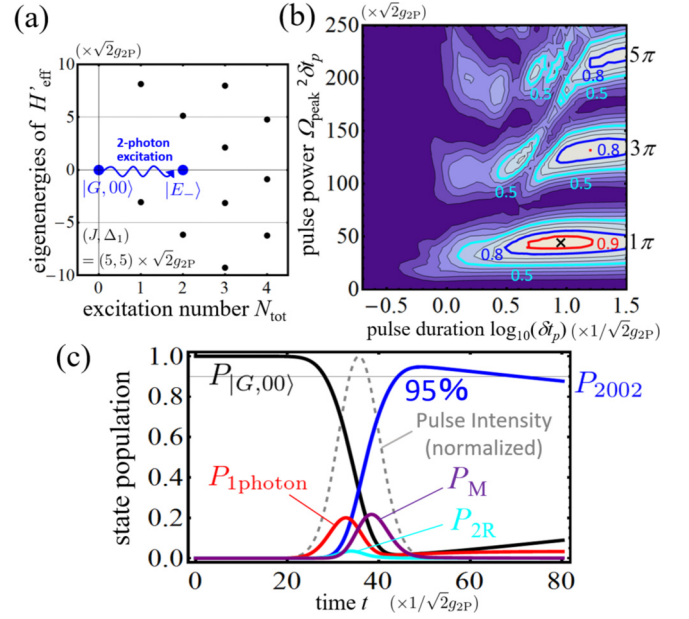


FIG. 5. (a) Set of eigenenergies and excitation number of the eigenstates of H'_{eff} in Eq. (10) for $(J, \Delta_1, \Delta_2, \omega_p - \omega_{2P}) = (5, 5, -0.05, -0.05)$. (b) Population of the 2002-GES (P_{2002}) generated just after the pulse excitation ($t = t_{\text{peak}} + 2\delta t_p$), as a function of pulse power $\Omega_{\text{peak}}^2 \delta t_p$ and pulse duration δt_p . (c) Rabi excitation dynamics (π pulse) for $(J, \Delta_1, \Delta_2, \omega_p - \omega_{2P}, \kappa) = (5, 5, -0.05, -0.05, 0.1) \times \sqrt{2}g_{2P}$ with $\Omega_{\text{peak}}^2 \delta t_p = 45 \times \sqrt{2}g_{2P}$ and $\delta t_p = 10^{0.95} / (\sqrt{2}g_{2P})$, corresponding to the parameters marked by a cross in (b). The half width at half maximum of the Rabi pulse intensity is $(\ln 2/2)^{1/2} \delta t_p \approx 0.59 \delta t_p$.

the state with $N_{\text{tot}} = 4$, whose eigenenergy of H'_{eff} is close to zero in Fig. 5(a), can be prevented considering the time scale of the excitation dynamics in Fig. 5(c)].

We perform a numerical simulation on the pulsed Rabi dynamics by solving Eq. (9), where the pulse shape is assumed to be a Gaussian function, $\Omega(t) = \Omega_{\text{peak}} \exp(-(t - t_{\text{peak}})^2 / \delta t_p^2)$. In Fig. 5(b), we plotted population of the 2002-GES generated just after the pulsed excitation, $P_{2002}|_{t=t_{\text{peak}}+2\delta t_p} \equiv \text{Tr}(|E_-\rangle\langle E_-| \times \rho(t_{\text{peak}} + 2\delta t_p))$, as a function of the pulse power ($\propto \Omega_{\text{peak}}^2 \delta t_p$) and the duration δt_p . We found several maxima located with almost equal intervals in the pulse power, with each corresponding to 1π , 3π , and 5π pulse conditions from the bottom of the plot. The highest probability exceeds 90% with π -pulse excitation. In order to have high probability, the pulse intensity should not be too strong (to avoid the higher-number state mixing), and the pulse duration should be shorter than the state decay time, $\delta t_p < 1/\Gamma_{2002}$ (Γ_{2002} will be given in Sec. II C), and longer than the tunneling time, $1/J < \delta t_p$. The last requirement comes from the fact that a short pulse duration results in the frequency broadening $1/\delta t_p$, degrading the success probability of the selective excitation of the targeted 2002-GES if the broadened linewidth exceeds the energy separation from other states, $O(J)$. In this way, there exists an optimal pulse duration. Figure 5(c) shows the dynamics of the state population with the optimal π -pulse excitation [corresponding to a cross in Fig. 5(b)]. In this case, population of the 2002-GES, P_{2002} , reaches 95% and population of the other two and higher number states, P_{2R}

and P_M , are suppressed to be less than 1%. Demonstrating the deterministic generation with high- Q nanocavities, especially with small $\kappa = 0.1 \times \sqrt{2}g_{2P}$ for Fig. 5(c) [i.e., $Q \approx 0.18 \times 10^6$ for $\omega_1 (\approx \omega_2) = 1.3$ eV and $g_{2P} = 50$ μ eV], is challenging in current technology but will be reached in the future [59,60].

To summarize this section, the 2002-GES can be exclusively excited in the system in both nondeterministic and deterministic ways by resonant laser excitation, if it is prepared as an eigenstate by tuning the cavity resonance to satisfy Eq. (5).

C. Decay of 2002-GES via cavity leakage

Once created by π -pulse excitation, population of the 2002-GES, $P_{2002} \equiv \text{Tr}(|E_s\rangle\langle E_s|\rho)$, gradually decreases with time due to free decay of photons from the cavity. Here we study in details the decay dynamics, which enables the evaluation of available rate of simultaneous two-photon detection (see Sec. IID).

The free decay dynamics is described by a closed set of rate equations for P_{2002} , $P_{1P,\pm} \equiv \text{Tr}(|1P,\pm\rangle\langle 1P,\pm|\rho)$, and $P_{G,00} \equiv \text{Tr}(|G,00\rangle\langle G,00|\rho)$, which is derived from Eq. (9) by neglecting population of the other states with two or more photons ($P_M = P_{2R} = 0$):

$$\frac{d}{dt}P_{2002} = -\Gamma_{2002}P_{2002}, \quad (14)$$

$$\frac{d}{dt}P_{1P,\pm} = (\Gamma_{2002}/2)P_{2002} - \Gamma_{1P,\pm}P_{1P,\pm}, \quad (15)$$

$$\frac{d}{dt}P_{G,00} = \Gamma_{1P,+}P_{1P,+} + \Gamma_{1P,-}P_{1P,-}, \quad (16)$$

where the decay rate $\Gamma_{2002} = 2(\sin \varphi_s)^2 \kappa$ and $\Gamma_{1P,\pm} = \kappa$. As it is clear from the expression of Γ_{2002} , the decay rate of the 2002-GES is reduced from the bare rate of two-photon states 2κ , by a factor $(\sin \varphi_s)^2$ which is the fraction of photonic component in $|E_s\rangle$ [whereas the biexcitonic fraction is $(\cos \varphi_s)^2$; see Eq. (6)]. In the case of the deterministic π -pulse generation, by solving the equations with $P_{2002} = 1$ and $P_{1P,\pm} = P_{G,00} = 0$ at $t = 0$, we found

$$\rho(t) = P_{2002}(t)|E_s\rangle\langle E_s| + \sum_{\sigma=\pm} P_{1P,\sigma}(t)|1P,\sigma\rangle\langle 1P,\sigma| + P_{G,00}(t)|G,00\rangle\langle G,00|, \quad (17)$$

where

$$P_{2002}(t) = e^{-\Gamma_{2002}t}, \quad (18)$$

$$P_{1P,\pm}(t) = \frac{\Gamma_{2002}(e^{-\Gamma_{1P,\pm}t} - e^{-\Gamma_{2002}t})}{2(\Gamma_{2002} - \Gamma_{1P,\pm})}, \quad (19)$$

$$P_{G,00}(t) = 1 - P_{2002} - P_{1P,+} - P_{1P,-}. \quad (20)$$

Long-time evolution of the population of the 2002-GES, P_{2002} , vacuum state, $P_{G,00}$, and one-photon state, $P_{1\text{photon}} (\equiv P_{1P,+} + P_{1P,-})$, are shown in Fig. 6, where exact numerical results (solid lines) are compared with analytic results in Eqs. (18)–(20). It clearly shows that the long-time scale dynamics is well approximated by the analytic result (for $t > 28t_p = 17.8 \times 1/\sqrt{2}g_{2P}$ when the Rabi excitation dynamics is negligible). One photon population $P_{1\text{photon}}$ initially

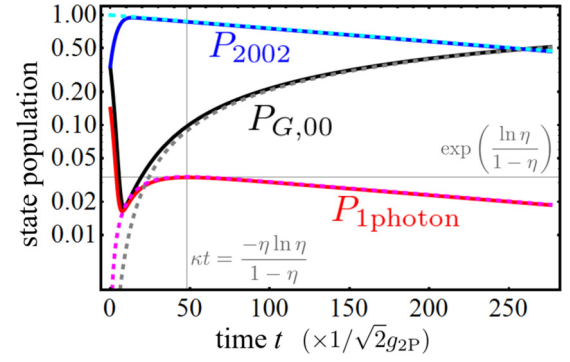


FIG. 6. Decay dynamics of the state population [long-time scale view of Fig. 5(c)]. We shift the origin of time ($t = 0$) to the pulse peak time [t_{peak} in Fig. 5(c)]. Solid and dashed lines show the numerical and analytic results [Eqs. (18)–(20)], respectively. From analytic solution, the maximum one-photon population $P_{1\text{photon}}$ is given by $\exp(\frac{\ln \eta}{1-\eta}) \approx 0.034$ (gray line), where $\eta = \Gamma_{2002}/\Gamma_{1P,\pm} = 2(\sin \varphi_s)^2 \approx 0.038$ in this plot.

increases and monotonically decreases with time after a peak time. By using Eq. (19) and $\eta \equiv \Gamma_{2002}/\Gamma_{1P,\pm} = 2(\sin \varphi_s)^2$, the peak time and peak values are approximated well by $\kappa^{-1} \frac{\ln \eta}{1-\eta}$ and $\exp(\frac{\ln \eta}{1-\eta})$, respectively. Thus one-photon probability can be made small by tuning Δ_1 so that η is small.

D. Two-photon simultaneous detection rate of emitted 2002-state photons

Here we discuss available simultaneous detection rate of two photons emitted from the 2002-GES, whose measurements can be used in quantum state tomography [given by Eq. (B1) in Appendix B] and also in the application to phase-sensitive quantum metrology. In experiments, the rate of the simultaneous photodetection is measured by the number of multiphoton counting events within a small time window, ΔT_w [37,61]. While the detection rate increases with ΔT_w , a visibility of the multiphoton interference will diminish due to an increase in the time uncertainty. An important quantity we discuss here is the maximum detection rate, at which the real quantum state tomography shows the NOON-state correlation correctly with sufficient visibility.

Under excitation of the 2002-GES with deterministic π pulse, the number of events for simultaneous detection of photons emitted from cavity i and j in a time window ΔT_w is

$$\begin{aligned} \mathcal{N}_{ij} &= \int \int \langle \hat{T}_+ \hat{T}_- \hat{I}_i(t) \hat{I}_j(t') \rangle \theta(\Delta T_w - |t - t'|) dt dt' \\ &= \kappa^2 \int_0^{t_f} dt \int_0^{\Delta T_w} d\tau (a_i^\dagger(t) a_j^\dagger(t+\tau) a_j(t+\tau) a_i(t) \\ &\quad + (i \leftrightarrow j)), \\ &= \kappa^2 \int_0^{t_f} dt \int_0^{\Delta T_w} d\tau \text{Tr}(a_j^\dagger a_j e^{\mathcal{L}|_{\Omega=0}\tau} [a_i \rho(t) a_i^\dagger]) \\ &\quad + (i \leftrightarrow j), \end{aligned} \quad (21)$$

where t_f is the accumulation time for photodetection, $\hat{I}_{i(j)}(t) = \kappa a_{i(j)}^\dagger(t) a_{i(j)}(t)$ is the Heisenberg operator of the emission rate from $i(j)$ th cavity at time t , $\theta(x)$ is the Heaviside step function,

$\hat{T}_{+(-)}$ is a time ordering (antiordering) operation applied to the Heisenberg operators of $a(a^\dagger)$, and $\langle \hat{X} \rangle \equiv \text{Tr}(\hat{X}\rho_0)$ with an initially prepared 2002-GES, $\rho_0 = |E_s\rangle\langle E_s|$. The time evolution of the density matrix, $\rho(t)$, is given by Eqs. (17)–(20). The accumulation time t_f is longer than the decay time of the 2002-GES, $t_f > 1/\Gamma_{2002}$, and is assumed equal to the pulse repetition time ΔT_{rep} for repeated-pulse measurements. In this case, t_f is replaced by $+\infty$ in Eq. (21). Under the assumption, the diagonal part of ρ_{tom} in Eq. (B1) can be expressed as

$$\mathcal{N}_{11} = \mathcal{N}_{22} = \kappa \int_0^{\Delta T_w} e^{-\kappa\tau} ((\cos\phi)^4 + (\sin\phi)^4 + 2(\sin\phi \cos\phi)^2 \cos(\Delta E_1\tau)) d\tau, \quad (22)$$

$$\mathcal{N}_{12} = 2\kappa \int_0^{\Delta T_w} (\sin\phi \cos\phi)^2 e^{-\kappa\tau} (1 - \cos(\Delta E_1\tau)) d\tau, \quad (23)$$

where $\Delta E_1 \equiv E_{1P,+} - E_{1P,-} = \sqrt{(\Delta_1 - \Delta_2)^2 + 4J^2}$. Similarly, we find an expression for the off-diagonal element ($\mathcal{N}_{1122} = \mathcal{N}_{2211}^*$) as

$$\begin{aligned} \mathcal{N}_{1122} &= \kappa^2 \int_0^{t_f} dt \int_0^{\Delta T_w} d\tau \langle a_1^\dagger(t) a_1^\dagger(t+\tau) a_2(t+\tau) a_2(t) \rangle \\ &= -\kappa \int_0^{\Delta T_w} e^{-\kappa\tau} (2(\sin\phi \cos\phi)^2 + (\cos\phi)^4) e^{-i\Delta E_1\tau} \\ &\quad + (\sin\phi)^4 e^{i\Delta E_1\tau} d\tau. \end{aligned} \quad (24)$$

From these results, the density matrix ρ_{tom} obtained by the state tomography is found to be the same as those for pure 2002 states if

$$\Delta T_w \ll 1/\Delta E_1. \quad (25)$$

Equation (25) can also be regarded as a condition for the “which-path” information of the emission frequencies to be erased [36,37,61,62]. With this short-time window,

$$\mathcal{N}_{11} = \mathcal{N}_{22} = -\mathcal{N}_{1122} = -\mathcal{N}_{2211}^* = \kappa \Delta T_w, \quad (26)$$

and all other elements including \mathcal{N}_{12} become zero to the leading order in $\Delta E_1 \Delta T_w$ ($\Delta E_1 \gg \kappa$ is already assumed). For the larger time window, $\Delta T_w > 1/\Delta E_1$, the photon correlation measurement does not reflect the initially prepared 2002-GES and the visibility of multiphoton interference decreases. The rapid oscillation terms with a frequency ΔE_1 in \mathcal{N}_{ij} and \mathcal{N}_{1122} arise from the coherent oscillation between $|G, 10\rangle$ and $|G, 01\rangle$, which takes place once the prepared 2002-GES ($|E_s\rangle$) emits one photon until the second photon is emitted.

From the above consideration, maximally available two-photon simultaneous detection rate $\mathcal{I}_{2002} (\equiv \mathcal{N}_{11}/\Delta T_{\text{rep}})$ is estimated to be

$$\mathcal{I}_{2002} = \frac{\kappa \Delta T_w}{\Delta T_{\text{rep}}} \leq \frac{\kappa \Gamma_{2002}}{\Delta E_1} = O\left(\frac{\kappa^2}{J} (\sin\phi_s)^2\right), \quad (27)$$

for $\Delta T_{\text{rep}} (= t_f) \geq 1/\Gamma_{2002}$. As an example, for parameters in Fig. 5(c) ($t, \Delta_1, \Delta_2, \kappa$) = (5, 5, -0.05, 0.1) $\times \sqrt{2} g_{2P}$ and $g_{2P} = 50 \mu\text{eV}$ ($g = 100 \mu\text{eV}$ and $\chi = 0.8 \text{ meV}$), the maximum

detection rate $\kappa \Gamma_{2002}/\Delta E_1$ is estimated to be 3.7 MHz. This rate is by three orders higher than those obtained by the SPDC-based source of kHz range used in Ref. [23].

To obtain further enhancement of the rate \mathcal{I}_{2002} , the dynamic Q switching in nanocavities [63] can be used, since high- Q cavities are required only for the energy-selective pure-state excitation discussed in Sec. II B and not for the two-photon emission and detection processes studied in this section. Deterministic and high-rate emission of the 2002-state photons will become possible by switching the Q factor ($Q \propto 1/\kappa$) from the high value ($\kappa \ll J$) to low value ($\kappa \gg J$) just after the π -pulse preparation. In this case, the maximally available rate is determined by the time scale of the two-photon Rabi dynamics, or the pulse duration δt_p which is larger than $1/J$ (see the discussion in Sec. II B). The estimation gives an upper limit of the rate of $O(J)$.

III. EXTENSION TO $N > 2$

Here we present extension of the above method to the general case of $N(>2)$. First, we describe a general recipe for NOON-state generation in Sec. III A. In Sec. III B, as an example of the extension, we use the recipe to find a design of the four-photon NOON-state generator, where numerical simulation clarifies the requirement for system parameters (cavity Q factor, detuning, coupling strength, etc.) to have pure NOON-state generation. The importance of step 2 in the recipe is highlighted in Sec. III C.

A. Recipe for NOON-state generation

As shown in the previous section for the case of $N = 2$, the key of our method was to prepare the target NOON state as an energy eigenstate. To do so, the quantum interference was utilized to eliminate the population in undesired states. In a similar manner, we can prepare NOON state in the eigenstate of the system. For clarity, we shall call such an energy eigenstate, which can generate output of NOON-state photons, “NOON-state generating eigenstate” and abbreviate it as NOON-GES. To prepare the NOON-GES for $N > 2$, we just have to follow our recipe below consisting of three steps.

Step 1. Consider N -photon emitter coupling to two-mode cavities. Here, N -photon emitter is defined as quantum emitter which permits simultaneous emission of N photons. A system with N_B QDs in biexciton state and N_X QDs in a single exciton state is N -photon emitter of $N = 2N_B + N_X$. (A system in Fig. 1 is two-photon emitter of $N = 2$, $N_B = 1$, and $N_X = 0$.) Define the system Hamiltonian, according to the types of the coupling between emitter and cavity modes.

Step 2. According to the Hamiltonian, draw schematic in the Hilbert subspace of N_{tot} (\equiv total number of photons and excitons) = N , which shows all directions of population flow at an initial time out from the prepared NOON-GES [Fig. 2(b) is the corresponding schematic for the system in Fig. 1]. The NOON-GES is a superposition state in the subspace of $N_{\text{tot}} = N$ which does not contain $|G, n N - n\rangle$ for $1 \leq n \leq N - 1$, where G represents a vacuum state of QDs with no exciton. In the schematic, if there exist multiple or no path of the flow into each state to be eliminated ($|G, n N - n\rangle$ for $1 \leq n \leq N - 1$),

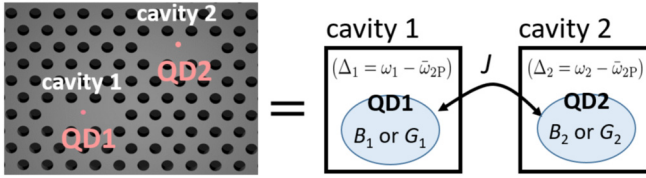


FIG. 7. Schematic of the QD-coupled nanocavity system (QD1 + QD2 + cavity 1 + cavity 2) for four-photon NOON state generation (right), which can be realized in a PhC platform (left).

the system can be considered as a candidate of NOON-state generator.

Step 3. For the candidate system (step 2), solve N -conditioned eigenvalue problem to find tuning parameters of the system so that the NOON-GES be an eigenstate of the Hamiltonian.

We should add more explanation on step 2. In the schematic, directions of population flow are drawn by taking the NOON-GES as an initial state. It indicates the unitary dynamics of the density matrix at an initial time from the NOON-GES. If the NOON-GES is the eigenstate of Hamiltonian, the density matrix should be conserved through the unitary dynamics. To realize this situation, the population flow into the other state ($|G, n \ N - n\rangle$ with $1 \leq n \leq N - 1$) must be eliminated. Presence of multiple or no path of the population flow into these unwanted states is a requirement so that the initially prepared NOON-GES can be conserved in the unitary dynamics. If multiple flows into each of the other states are present, they need to interfere destructively to cancel out, for which additional requirement is taken into account in step 3.

If the NOON-GES is contained as an eigenstate of the system, the resonant laser excitation can be used to generate it exclusively, being similar to the case of $N = 2$. In the following subsection, we apply this recipe to 4004-state generation as an example.

B. Example: 4004-state generation

As an example, here we show that it is possible to generate 4004 state using the recipe shown in the previous subsection.

Step 1. We consider a system with two QDs, QD1 and QD2, in cavity 1 and cavity 2, respectively (Fig. 7). We assume that the interaction between the QDs and cavities occurs only through the biexciton-two photon transitions, in the same way as the 2002-state generator. Therefore, this system is categorized by $N = 4$, $N_B = 2$, and $N_X = 0$ in recipe (i). The biexciton two-photon resonance frequency in QD1 (QD2) is $\omega_{2P,1(2)} \approx \omega_{X_{1(2)}} - \chi_{1(2)}/2$. State vectors are given by $|i_1 i_2\rangle \otimes |n_1 n_2\rangle$, where $i_1 \in \{B_1, G_1\}$ ($i_2 \in \{B_2, G_2\}$) represents the QD carrier states in QD1 (QD2), and $|n_1 n_2\rangle$ is a photon number state with $n_{1(2)}$ photons inside cavity 1(2). B_j and G_j ($j = 1, 2$) are biexciton and vacuum states in the j th QD. Alternatively, we define more simple notation for the QD carrier states: $|Q\rangle \equiv |B_1, B_2\rangle$, $|B1\rangle \equiv |B_1, G_2\rangle$, $|B2\rangle \equiv |G_1, B_2\rangle$, and $|G\rangle \equiv |G_1, G_2\rangle$. With this notation, the total number of excitation is given by $N_{\text{tot}} = 4|Q\rangle\langle Q| + 2(|B1\rangle\langle B1| + |B2\rangle\langle B2|) + a_1^\dagger a_1 + a_2^\dagger a_2$.

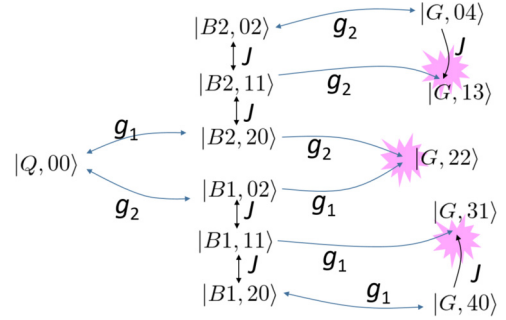


FIG. 8. Population flow at an initial time, shown in the Hilbert subspace of $N_{\text{tot}} = 4$ for the model system in Fig. 7, starting from the prepared 4004-GES, i.e., Eq. (29) with Eqs. (30)–(33).

The effective Hamiltonian in a frame rotating with the mean biexciton two-photon resonance frequency, $\bar{\omega}_{2P} (\equiv \frac{\omega_{2P,1} + \omega_{2P,2}}{2})$, $H_{\text{eff}} = H - \bar{\omega}_{2P} N_{\text{tot}}$, is given by

$$H_{\text{eff}} = \sum_{j=1,2} \Delta_j a_j^\dagger a_j + J(a_1^\dagger a_2 + a_2^\dagger a_1) + \Delta_B (|B1\rangle\langle B1| - |B2\rangle\langle B2|) + \sum_{j=1,2} g_j (a_j^2 |B_j\rangle\langle G_j| + |G_j\rangle\langle B_j| (a_j^\dagger)^2), \quad (28)$$

where $\Delta_j (\equiv \omega_j - \bar{\omega}_{2P})$ is the cavity detuning and $\Delta_B (\equiv \omega_{2P,1} - \omega_{2P,2})$ is the difference in the biexciton two-photon resonance frequencies. Regarding g_1 as the unit of energy, there are five free parameters in the Hamiltonian which determine the system dynamics: $(g_2/g_1, J/g_1, \Delta_1/g_1, \Delta_2/g_1, \Delta_B/g_1)$.

Step 2. Based on the Hamiltonian H_{eff} , we indicate the direction of population flow as shown in Fig. 8, in the Hilbert subspace $N_{\text{tot}} = 4$. We found two paths of flow into $|G, 13\rangle$, $|G, 22\rangle$, and $|G, 31\rangle$, respectively. Therefore, this system can be a candidate of the 4004-state generator.

Step 3. In this step, we will find the parameter values with which the 4004-GES is contained as one of the four photon eigenstates $|E\rangle$ of H_{eff} , by solving the eigenproblem $H_{\text{eff}}|E\rangle = E|E\rangle$. The four photon eigenstate is expanded by 12 states which appear in Fig. 8:

$$|E\rangle \equiv A_{Q,00}|Q,00\rangle + \sum_{n_1+n_2=2} A_{B1,n_1n_2}|B1,n_1n_2\rangle + \sum_{n_1+n_2=2} A_{B2,n_1n_2}|B2,n_1n_2\rangle + \sum_{n_1+n_2=4} A_{G,n_1n_2}|G,n_1n_2\rangle, \quad (29)$$

for which we assign four requirements to be the 4004-GES,

$$A_{G,31} = 0, \quad (30)$$

$$A_{G,22} = 0, \quad (31)$$

$$A_{G,13} = 0, \quad (32)$$

$$|A_{G,40}| = |A_{G,04}|. \quad (33)$$

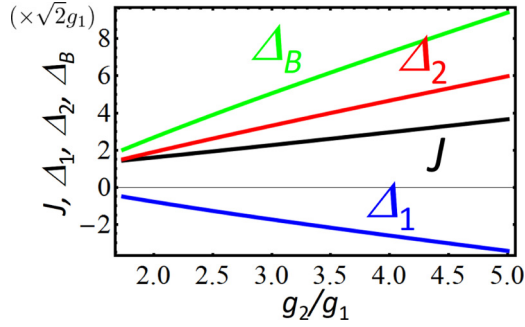


FIG. 9. Parameters with which the 4004-GES becomes one of the four-photon eigenstates $|E\rangle$ of H_{eff} for the model in Fig. 7: J (black), Δ_1 (blue), Δ_2 (red), and Δ_B (green).

Inserting the first three conditions, Eq. (30)–(32), into the eigenequation, they explicitly read

$$0 = \sqrt{4}JA_{G,04} + \sqrt{6}g_2A_{B2,11}, \quad (34)$$

$$0 = \sqrt{2}g_2A_{B2,20} + \sqrt{2}g_1A_{B1,02}, \quad (35)$$

$$0 = \sqrt{6}g_1A_{B1,11} + \sqrt{4}JA_{G,40}. \quad (36)$$

These are understood as three requirements for these multiple quantum processes to vanish, in a fully destructive way, the production rate of unwanted states ($|G,31\rangle$, $|G,22\rangle$, and $|G,13\rangle$). The four requirements [Eqs. (33)–(36)] fix the four free parameters ($J/g_1, \Delta_1/g_1, \Delta_2/g_1, \Delta_B/g_1$) with g_2/g_1 remaining as one free parameter. Thanks to the symmetry of this system with respect to the exchange, (cavity 1, QD1) \leftrightarrow (cavity 2, QD2), we can restrict our analysis, without loss of generality, to the reduced parameter space, $g_2/g_1 \geq 1$. We found numerically a solution to the conditional eigenvalue equation for $g_2/g_1 \geq 1.74$, for which the parameter values are shown in Fig. 9.

For parameters satisfying these requirements, the 4004-GES, $|E_{4004}\rangle$, and the energy, E_{4004} , are given by

$$|E_{4004}\rangle = A_{4004} \left(\frac{|G,40\rangle - |G,04\rangle}{2} \right) + A_{Q,00}|Q,00\rangle + \sum_{l=B1,B2} \sum_{n_1+n_2=2} A_{l,n_1n_2}|l,n_1n_2\rangle, \quad (37)$$

$$E_{4004} = \frac{6\Delta_1 + \Delta_B}{2} + \sqrt{\left(\Delta_1 - \frac{\Delta_B}{2}\right)^2 + 6g_1^2 - 4J^2} \\ = \frac{6\Delta_2 - \Delta_B}{2} - \sqrt{\left(\Delta_2 + \frac{\Delta_B}{2}\right)^2 + 6g_2^2 - 4J^2}. \quad (38)$$

We notice that $|E_{4004}\rangle$ contains also the photon number states with less than four photons, which, however, do not contribute to simultaneous four-photon detection and hence do not affect ρ_{tomo} reconstructed by four-photon quantum state tomography.

Evaluation of purity and detection rate of the 4004-state emission. In order to evaluate the purity of emitted 4004-state photons, we study ρ_{tomo} and concurrence $\mathcal{C}(\equiv |\langle 40|\rho_{\text{tomo}}|04\rangle|)$ in a similar manner as presented in Sec. II B. The simulation is performed for weak cw laser excitation on cavity 1 with $H_{\text{pump}} = \Omega(a_1 + a_1^\dagger)$, under the resonance condition,

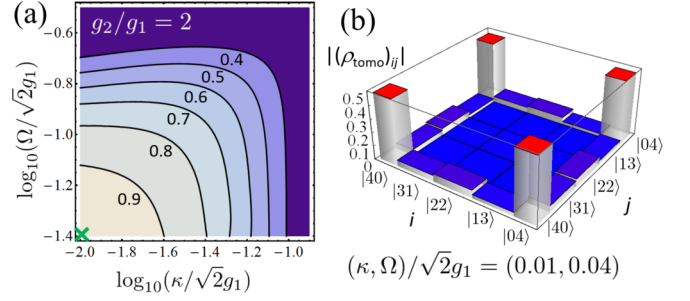


FIG. 10. (a) Simulated concurrence \mathcal{C} of the emission from the model in Fig. 7, shown as a function of (κ, Ω) for $g_2/g_1 = 2$ and $(J, \Delta_1, \Delta_2, \Delta_B) = (1.61, -0.78, 1.90, 2.68) \times \sqrt{2}g_1$ (see Fig. 9). (b) Four-photon density matrix ρ_{tomo} , which will be constructed by quantum state tomography for $(\kappa, \Omega) = (0.01, 0.04) \times \sqrt{2}g_1$ [corresponding to a cross in (a)].

$\omega_p - \bar{\omega}_{2P} = E_{4004}/4$ (pumping on cavity 2 can also be used here, see Appendix A). Figure 10(a) shows the simulated concurrence \mathcal{C} plotted as a function of (κ, Ω) for a set of parameters satisfying Eqs. (33)–(36): $g_2/g_1 = 2$ and $(J, \Delta_1, \Delta_2, \Delta_B) = (1.61, -0.78, 1.90, 2.68) \times \sqrt{2}g_1$ (see Fig. 9). Being similar to the case of 2002-state (Fig. 5), high concurrence, $\mathcal{C} > 0.9$ is obtained only for high- Q cavity (small κ) and weak pumping (small Ω). Figure 10(b) is the simulated ρ_{tomo} for $(\kappa, \Omega) = (0.01, 0.04) \times \sqrt{2}g_1$, which is close to that of a pure 4004 state. However, demonstrating such a device with $\kappa = 0.01 \times \sqrt{2}g_1$ (i.e. $Q \approx 1.8 \times 10^6$ for $\omega_1 (\approx \omega_2) = 1.3$ eV and $g_1 = 50$ μeV) is highly challenging with current state-of-the-art technology.

Compared to 2002-state generation, much higher quality factor of cavities is necessary to have high \mathcal{C} . This indicates that the generation rate of pure 4004 state is reduced more strongly than those of the 2002 state. From an analogy with the discussion on detection rate of the 2002 states, the maximally available rate of four-photon simultaneous detection is estimated to be $\propto \kappa(\kappa/J)^3$. However, this rate can be largely improved by using Q -switching technique, in a similar manner as discussed for 2002-state generator in Sec. II D.

C. Significance of step 2

Step 2 of the recipe is useful as a general guideline to judge in a simple way (without any calculation) to which types of system configurations we can apply our scheme to design efficient $N00N$ -state generator. As a simple example, we discuss the case of 4004 state generation.

The system shown in Fig. 7 successfully becomes 4004-state emitter if system parameters are properly chosen. With the same elements, two QDs and two cavities ($N = 4$, $N_B = 2$, and $N_X = 0$), there is another system configuration as shown in Fig. 11(a). The only difference from Fig. 7 is in the location of QDs. However, by following step 2 of the recipe, we can see the system cannot be a candidate for 4004-state generator with our method. To see this, we just have to draw schematic as shown in Fig. 11(b), showing all population flows at an initial time out from the prepared 4004-GES, according to the Hamiltonian [in which the QD-cavity interaction term is

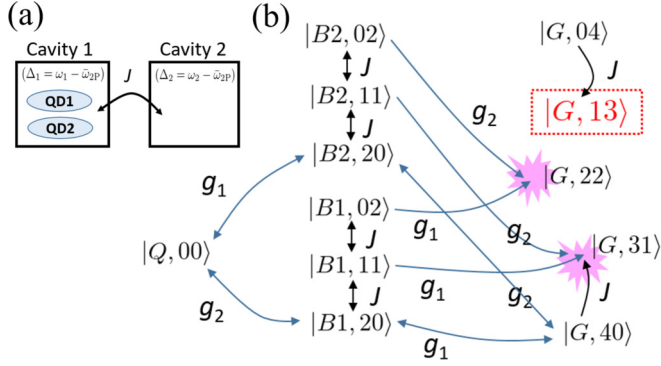


FIG. 11. (a) Two QDs in coupled-cavity system with a system configuration different from Fig. 8 (QDs emit photons to cavity 1 only through the biexciton two-photon transitions). (b) Coherent population flow at an initial time starting from prepared 4004-GES, i.e., Eq. (29) with Eqs. (30)–(33), for the system shown in (a). According to the recipe (step 2), the 4004-GES state cannot be included as an eigenstate in this system. Therefore, this system cannot be the 4004-state generator with our method.

replaced as $a_j^2 \rightarrow a_1^2$ and $(a_j^\dagger)^2 \rightarrow (a_1^\dagger)^2$ in Eq. (28)]. In the figure, we find multiple paths to $|G, 22\rangle$ and $|G, 31\rangle$ which are required to be eliminated for 4004-state generation. Full vanishing of the production rates for these two states is made possible by choosing parameters so that the multiple quantum paths interfere destructively. This can be done by assigning two requirements,

$$0 = \sqrt{2}g_2 A_{B2,02} + \sqrt{2}g_1 A_{B1,20}, \quad (39)$$

$$0 = \sqrt{6}g_2 A_{B2,11} + \sqrt{6}g_1 A_{B1,11} + \sqrt{4}J A_{G,40}, \quad (40)$$

to the four-photon eigenequation. On the other hand, there is only one population flow into $|G, 13\rangle$ [enclosed by dotted square in Fig. 11(b)]. Therefore, the destructive interference cannot be used and the production rate does not vanish. In this way, we can conclude the system in Fig. 11(a) is not a candidate of the 4004-state generator, irrespective of the parameters chosen. The situation is clearly different from the one shown in Fig. 8. Of course, this test (step 2) is cleared in the above-discussed 2002-state generator, and also in polarization-entangled 2002-state emitter [36].

IV. CONCLUSIONS

In this paper, we proposed a generation method of photonic NOON state with QDs in coupled nanocavities. Starting from $N = 2$, we show our recipe to generate NOON-state photons for $N > 2$. The key of our method is to find the system parameters so that the NOON-state generating state “NOON-GES” can be prepared as an energy eigenstate of the system. This is possible when multiple quantum paths can be used to eliminate perfectly the production rate of the unwanted states ($|G, n_1 n_2\rangle$ with $n_1 + n_2 = N$ and $1 \leq n_1 \leq N - 1$). In the presence of the strong nonlinearity, the NOON-GES can be resonantly excited, and the NOON-state photons can be emitted and observed by simultaneous multiphoton detection.

To excite NOON-GES exclusively (to observe high concurrence \mathcal{C} and small trace distance \mathcal{D} from the pure state) through resonant pumping, the linewidth (or decay rate) of the NOON-GES needs to be small. Therefore, high- Q cavities are required in this method. This reduces the efficiency of multiphoton simultaneous emission and detection rates of the NOON-state photons, $\mathcal{I}_{\text{NOON}}$, which follow a scaling law, $\mathcal{I}_{\text{NOON}} \propto \kappa(\kappa/J)^{N-1}$. Even if we take into account the limitation, the available detection rate in our 2002-state generator is estimated to be by three orders higher than those obtained with the typical 2002-state photon source [23]. Moreover, by utilizing the Q -switching technique [63], further enhancement in the emission rate will become possible (the emission can even become deterministic for the 2002-state generator).

We mention here the dephasing effect of the QD excitons (say γ_{phase}), which was simply neglected in the analysis. The most dominant effect will come from that for the biexciton state (not for the single-exciton state) for the NOON-state generator using the biexciton-two-photon resonance. Given that the π -pulse excitation of 2002-GES is successfully achieved, the population decay dynamics and the two-photon detection rate (in Secs. II C and II D) are unaffected by the presence of the dephasing. The reason for the latter is that the fast oscillation terms in the τ dependency, e.g., in Eq. (21), attribute solely to the dynamics of the one-photon states with no QD exciton. As for the π -pulse excitation, the Rabi excitation dynamics can be made fast enough to be completed before the QD biexciton can dephase, if $\gamma_{\text{phase}} < O(J) = O(g_{2P})$. Considering the rough estimation, $g_{2P} = 50 \mu\text{eV}$, the last requirement is fulfilled and thus we can use our scheme robustly, as far as the dephasing is not too strong. Of course, we cannot apply the discussion directly to the general case of NOON-state generator with $N > 2$. In this case, we can set the detection time window as $\Delta T_w < 1/\gamma_{\text{phase}}$ so that the dephasing effect is reduced in the multiphoton detection.

We also mention the difference between our method and the previously reported method for polarization-entangled two-photon NOON state [36,37]. As discussed above, the key of our method is to prepare NOON-GES as an energy eigenstate, while the previous method relies on the spontaneous emission of the prepared biexciton state into degenerate two polarization modes. Therefore, the previous method requires high symmetry between different polarization modes, i.e., pure 2002 state is generated when two cavity modes have the same strength in the biexciton-two-photon coupling and the same frequency at the biexciton-two-photon resonance. On the other hand, with our method, it is possible to generate pure 2002-state photons even if their coupling strengths are different, as far as the requirement in Eq. (5) is fulfilled.

Our method also has a disadvantage. The NOON-state generator proposed here requires high- Q cavity, strong coupling g , and high-precision tuning of cavity resonance. The realization becomes harder and harder as N increases. Further optimization of the system design, including the parameter choice in combination with frequency filtering [37,64], will increase the quality of the emitted NOON-state photons, and hence could relax the requirements, the details of which we leave as a future issue.

ACKNOWLEDGMENTS

We thank T. Horikiri, M. Yamaguchi, M. Bamba, and M. Holmes for useful comments and discussions. This work was supported by the JSPS KAKENHI (Grants No. 15H05700 and No. 15K20931), the Project for Developing Innovation Systems of MEXT, and New Energy and Industrial Technology Development Organization (NEDO).

APPENDIX A: SELECTION RULE IN RESONANT TWO-PHOTON EXCITATION SPECIFIC TO THE 2002-STATE GENERATOR

In Sec. II B, we see that the 2002-GES, $|E_s\rangle$, can be excited by resonant laser field applied to cavity 2, $H_{\text{pump},2} = \Omega(a_2 + a_2^\dagger)$, but not to cavity 1. Actually, we confirmed by numerical simulation that resonant excitation on cavity 1, by replacing the pump Hamiltonian with $H_{\text{pump}} = \Omega(a_1 + a_1^\dagger)$, cannot generate the target 2002-state photons. Here, we show that it is due to an underlying selection rule for resonant two-photon excitation, which is specific to this 2002 generator. (As for the 4004 generator in Sec. III B, we confirmed numerically that the target 4004-state photons can be generated for each case with resonant laser field on cavity 1 or cavity 2.) This is an interesting physics (possibly with some application), which is out of the main scope of this paper.

In order to see this, we apply second-order perturbation theory based on Schrieffer-Wolff transformation [49,65] to find the effective Hamiltonian, $\tilde{\mathcal{H}} = e^S \mathcal{H} e^{-S}$, and the two-photon transition matrix element, $\langle E_s | \tilde{\mathcal{H}} | G, 00 \rangle$. To construct the effective Hamiltonian, we focus on the Hilbert subspace spanned by four eigenstates, the vacuum state, $|G, 00\rangle$, 2002-GES, $|E_s\rangle$, and two one-photon states, $|1P, \pm\rangle$. The other three two-photon eigenstates are energetically separated from the 2002-GES and hence are not considered here [e.g., in Fig. 5(a), two of them are shown at $N_{\text{tot}} = 2$ and another is outside the plot range).

First, we divide the Hamiltonian (in the rotating frame with the excitation laser frequency) into two terms, $\mathcal{H} = H_0 + V$: the unperturbed term,

$$H_0 = 0 \cdot |G, 00\rangle \langle G, 00| + (E_s - 2(\omega_p - \omega_{2P})) |E_s\rangle \langle E_s| + \sum_{\sigma=\pm} (E_{1P,\sigma} - (\omega_p - \omega_{2P})) |1P, \sigma\rangle \langle 1P, \sigma|, \quad (\text{A1})$$

and perturbation term, $V = V_1$ or V_2 with $V_{1(2)} = \Omega(a_{1(2)} + a_{1(2)}^\dagger)$. Using Schrieffer-Wolff transformation [49,65], the general form of the effective Hamiltonian up to the second order in V is

$$\tilde{\mathcal{H}} \approx H_0 + \sum_{i,f} M_{fi} |f\rangle \langle i|, \quad (\text{A2})$$

$$M_{fi} = \sum_k \frac{\langle f | V | k \rangle \langle k | V | i \rangle}{2} \left(\frac{1}{E_f - E_k} + \frac{1}{E_i - E_k} \right), \quad (\text{A3})$$

where $H_0 |m\rangle = E_m |m\rangle$ for $m = i, f, k$. The matrix element for the two-photon transition to the target 2002-GES under the resonant excitation [$E_s - 2(\omega_p - \omega_{2P}) = 0$] is obtained by putting the initial state $|i\rangle = |G, 00\rangle$, final target state

$|f\rangle = |E_s\rangle$, and two intermediate states $|k\rangle = |1P, \sigma (= \pm)\rangle$ into Eq. (A3).

Following straightforward calculation, we found the two-photon transition matrix element, for resonant pumping on cavity 2 ($V = V_2$),

$$M_{fi} = \sin \varphi_s \times \Omega^2 \times \left(\frac{(\sin \phi)^2}{E_{1P,+} - (\omega_p - \omega_{2P})} + \frac{(\cos \phi)^2}{E_{1P,-} - (\omega_p - \omega_{2P})} \right), \quad (\text{A4})$$

while for resonant pumping on cavity 1 ($V = V_1$),

$$M_{fi} = -\sin \varphi_s \times \Omega^2 \times \left(\frac{(\cos \phi)^2}{E_{1P,+} - (\omega_p - \omega_{2P})} + \frac{(\sin \phi)^2}{E_{1P,-} - (\omega_p - \omega_{2P})} \right). \quad (\text{A5})$$

The two terms in the brackets in Eq. (A4) and Eq. (A5) correspond to the contribution from two transition paths via two intermediate states $|1P, \pm\rangle$. Using the condition for cavity and laser frequencies, $\omega_p - \omega_{2P} = \Delta_2 = E_s/2$, and definition for ϕ below Eq. (12) (see Sec. II A and Sec. II B), we found the two contributions perfectly cancel with each other in Eq. (A5), leading to $M_{fi} = 0$ for the pumping on cavity 1 ($V = V_1$). On the other hand, this is not the case, $M_{fi} \neq 0$, for the pumping on cavity 2 ($V = V_2$). The result clearly shows existence of a selection rule for the two-photon resonant excitation: excitation of the 2002-GES through cavity pumping is allowed only via cavity 2, but forbidden via cavity 1.

APPENDIX B: METHOD OF SIMULATION FOR STATE TOMOGRAPHY, TRACE DISTANCE, AND CONCURRENCE

Here, the method of numerical calculation is briefly summarized. The two-photon density matrix ρ_{tomo} , which can be experimentally reconstructed by the quantum state tomography [36,37,61,66], is obtained from the two-photon correlation functions,

$$\rho_{\text{tomo}} = \mathcal{Z} \begin{pmatrix} \langle \frac{a_1^\dagger a_1^\dagger a_1 a_1}{2} \rangle & \langle \frac{a_1^\dagger a_1^\dagger a_2 a_1}{\sqrt{2}} \rangle & \langle \frac{a_1^\dagger a_1^\dagger a_2 a_2}{2} \rangle \\ \langle \frac{a_1^\dagger a_2^\dagger a_1 a_1}{\sqrt{2}} \rangle & \langle a_1^\dagger a_2^\dagger a_2 a_1 \rangle & \langle \frac{a_1^\dagger a_2^\dagger a_2 a_2}{\sqrt{2}} \rangle \\ \langle \frac{a_2^\dagger a_2^\dagger a_1 a_1}{2} \rangle & \langle \frac{a_2^\dagger a_2^\dagger a_2 a_1}{\sqrt{2}} \rangle & \langle \frac{a_2^\dagger a_2^\dagger a_2 a_2}{2} \rangle \end{pmatrix}, \quad (\text{B1})$$

where $\langle X \rangle \equiv \text{Tr}(X\rho)$ and \mathcal{Z} is a normalization factor to give $\text{Tr}(\rho_{\text{tomo}}) = 1$. Each component of the matrix is measured by simultaneous two-photon countings. Concurrence, $\mathcal{C} (\equiv 2|(\rho_{\text{tomo}})_{1,3}|)$, is an entanglement measure, given by the off-diagonal matrix element of ρ_{tomo} . This measure becomes unity for pure 2002 states [67],

$$\rho_{2002,\theta} = \frac{(|20\rangle + e^{-i\theta}|02\rangle)(\langle 20| + e^{i\theta}\langle 02|)}{2}. \quad (\text{B2})$$

The trace distance, \mathcal{D} , is defined by $\mathcal{D} \equiv \text{Tr}|\rho_{2002,\theta} - \rho_{\text{tomo}}| = \text{Tr}\sqrt{(\rho_{2002,\theta} - \rho_{\text{tomo}})^\dagger (\rho_{2002,\theta} - \rho_{\text{tomo}})}$. This is a measure indicating how close to a pure 2002 state the observed photons are, where $\mathcal{D} = 0$ means that the system emits exactly the pure 2002-state photons. In the simulation, the phase $\theta (\approx \pi)$ is chosen to minimize \mathcal{D} .

**APPENDIX C: TWO-PHOTON EMISSION RATE
OF THE 2002-STATE GENERATOR UNDER
WEAK cw LASER PUMPING**

By using the result in Appendix A, we obtain an approximate analytic expression for the two-photon emission rate of the 2002-state generator in the case of weak cw excitation (via cavity 2). The effective Hamiltonian is

$$\tilde{\mathcal{H}} \approx \xi(|G,00\rangle\langle E_s| + |E_s\rangle\langle G,00|) + \sum_{\sigma=\pm} (E_{1P,\sigma} - (\omega_p - \omega_{2P}))|1P,\sigma\rangle\langle 1P,\sigma|, \quad (\text{C1})$$

where we used the above result for the two-photon transition amplitude, $\xi \equiv M_{fi}$ in Eq. (A4) in Appendix A, and neglected the slight energy shift in the diagonal part of $\tilde{\mathcal{H}}$ for simplicity. Using this simple Hamiltonian, we found a steady-state solution to the quantum master equation, $\dot{\rho} = -i[\tilde{\mathcal{H}}, \rho] + \mathcal{L}_{\text{loss}}\rho = 0$, in analytic form (see the main text for

the definition of $\mathcal{L}_{\text{loss}}$). For the steady state, excited population of the 2002-GEN is

$$P_{2002} = 4\xi^2 / \Gamma_{2002}^2 \quad (\text{C2})$$

to the leading order in ξ , where $\Gamma_{2002} = 2(\sin\varphi_s)^2\kappa$ is the decay rate. The result is directly related to the rate of simultaneous two-photon emission (detected within a time window ΔT_w of relative delay) from the same cavity,

$$\begin{aligned} \mathcal{I}_{2002} &= \kappa^2 \Delta T_w (a_1^{\dagger 2} a_1^2 + a_2^{\dagger 2} a_2^2) \\ &= 2\kappa^2 \Delta T_w (\sin\varphi_s)^2 P_{2002} \\ &= 8\kappa^2 \Delta T_w (\sin\varphi_s)^2 \xi^2 / \Gamma_{2002}^2, \end{aligned} \quad (\text{C3})$$

where the time window is assumed small for the detector. The analytic result explains the high contrast in the peak emission intensity found at the two conditions, $\Delta_2 = E_{\pm}/2$, in Fig. 3 (dashed line).

-
- [1] R. J. Glauber, *Phys. Rev.* **130**, 2529 (1963).
[2] L. Mandel and E. Wolf, *Optical Coherence and Quantum Optics* (Cambridge University Press, Cambridge, England, 1995).
[3] E. Knill, R. Laflamme, and G. J. Milburn, *Nature (London)* **409**, 46 (2001).
[4] P. Kok, W. J. Munro, K. Nemoto, T. C. Ralph, J. P. Dowling, and G. J. Milburn, *Rev. Mod. Phys.* **79**, 135 (2007).
[5] S. Aaronson and A. Arkhipov, *Theory Comput.* **9**, 143 (2013).
[6] C. H. Bennett and G. Brassard, in *Proceedings of the IEEE International Conference on Computers, Systems and Signal Processing, Bangalore, India, 1984* (IEEE, New York, 1984), pp. 175–179; IBM Tech. Discl. Bull. **28**, 3153 (1985).
[7] C. H. Bennett, F. Bessette, G. Brassard, L. Salvail, and J. Smolin, *J. Cryptol.* **5**, 3 (1992).
[8] E. Waks *et al.*, *Nature (London)* **420**, 762 (2002).
[9] K. Takemoto, Y. Nambu, T. Miyazawa, Y. Sakuma, T. Yamamoto, S. Yoroizu, and Y. Arakawa, *Sci. Rep.* **5**, 14383 (2015).
[10] W. Denk, J. H. Strickler, and W. W. Webb, *Science* **248**, 73 (1990).
[11] N. Horton *et al.*, *Nat. Photon.* **7**, 205 (2013).
[12] N. Sim, M. F. Cheng, D. Bessarab, C. M. Jones, and L. A. Krivitsky, *Phys. Rev. Lett.* **109**, 113601 (2012).
[13] N. M. Phan, M. F. Cheng, D. A. Bessarab, and L. A. Krivitsky, *Phys. Rev. Lett.* **112**, 213601 (2014).
[14] P. Ball, *Nature (London)* **474**, 272 (2011).
[15] C. S. Muñoz, E. del Valle, A. G. Tudela, K. Müller, S. Lichtmannecker, M. Kaniber, C. Tejedor, J. J. Finley, and F. P. Laussy, *Nat. Photon.* **8**, 550 (2014).
[16] J. C. L. Carreño, and F. P. Laussy, *Phys. Rev. A* **94**, 063825 (2016).
[17] J. Dowling, *Contemp. Phys.* **49**, 125 (2008).
[18] A. N. Boto, P. Kok, D. S. Abrams, S. L. Braunstein, C. P. Williams, and J. P. Dowling, *Phys. Rev. Lett.* **85**, 2733 (2000).
[19] J. L. O’Brien, A. Furusawa, and J. Vučković, *Nat. Photon.* **3**, 687 (2009).
[20] V. Giovannetti, S. Lloyd, and L. Maccone, *Nat. Photon.* **5**, 222 (2011).
[21] T. Ono, R. Okamoto, and S. Takeuchi, *Nat. Commun.* **4**, 2426 (2013).
[22] P. Kok, S. L. Braunstein, and J. P. Dowling, *J. Opt. B: Quantum Semiclass.* **6**, s811 (2004).
[23] T. Nagata, R. Okamoto, J. L. O’Brien, K. Sasaki, and S. Takeuchi, *Science* **316**, 726 (2007).
[24] H. Wang, M. Mariani, R. C. Bialczak, M. Lenander, E. Lucero, M. Neeley, A. D. O’Connell, D. Sank, M. Weides, J. Wenner, T. Yamamoto, Y. Yin, J. Zhao, J. M. Martinis, and A. N. Cleland, *Phys. Rev. Lett.* **106**, 060401 (2011).
[25] Q.-P. Su, C.-P. Yang, and S.-B. Zheng, *Sci. Rep.* **4**, 3898 (2014).
[26] P. G. Kwiat, K. Mattle, H. Weinfurter, A. Zeilinger, A. V. Sergienko, and Y. H. Shih, *Phys. Rev. Lett.* **75**, 4337 (1995).
[27] P. Kok, H. Lee, and J. P. Dowling, *Phys. Rev. A* **65**, 052104 (2002).
[28] H. F. Hofmann and T. Ono, *Phys. Rev. A* **76**, 031806(R) (2007).
[29] I. Afek, O. Ambar, and Y. Silberberg, *Science* **328**, 879 (2010).
[30] S. Buckley, K. Rivoire, and J. Vučković, *Rep. Prog. Phys.* **75**, 126503 (2012).
[31] E. M. Purcell, *Phys. Rev.* **69**, 37 (1946).
[32] D. Englund, D. Fattal, E. Waks, G. Solomon, B. Zhang, T. Nakaoka, Y. Arakawa, Y. Yamamoto, and J. Vučković, *Phys. Rev. Lett.* **95**, 013904 (2005).
[33] S. Strauf *et al.*, *Nat. Photon.* **1**, 704 (2007).
[34] M. Nomura, N. Kumagai, S. Iwamoto, Y. Ota, and Y. Arakawa, *Nat. Phys.* **6**, 279 (2010).
[35] K. Kamide, S. Iwamoto, and Y. Arakawa, *Phys. Rev. Lett.* **113**, 143604 (2014).
[36] S. Schumacher *et al.*, *Opt. Express* **20**, 5335 (2012).
[37] E. del Valle, *New J. Phys.* **15**, 025019 (2013).
[38] M. Bayer, T. Gutbrod, J. P. Reithmaier, A. Forchel, T. L. Reinecke, P. A. Knipp, A. A. Dremin, and V. D. Kulakovskii, *Phys. Rev. Lett.* **81**, 2582 (1998).
[39] J. R. Reithmaier, G. Sek, A. Löffler, C. Hofmann, S. Kuhn, S. Reitzenstein, L. V. Keldysh, V. D. Kulakovskii, T. L. Reinecke, and A. Forchel, *Nature (London)* **432**, 197 (2004).
[40] S. M. de Vasconcellos, A. Calvar, A. Dousse, J. Suffczynski, N. Dupuis, A. Lemaitre, I. Sagnes, J. Bloch, P. Voisin, and P. Senellart, *Appl. Phys. Lett.* **99**, 101103 (2011).

- [41] S. Ishii and T. Baba, *Appl. Phys. Lett.* **87**, 181102 (2005).
- [42] A. Majumdar, A. Rundquist, M. Bajcsy, and J. Vučković, *Phys. Rev. B* **86**, 045315 (2012).
- [43] Y. Sato, Y. Tanaka, J. Upham, Y. Takahashi, T. Asano, and S. Noda, *Nat. Photon.* **6**, 56 (2012).
- [44] A. Majumdar, A. Rundquist, M. Bajcsy, V. D. Dasika, S. R. Bank, and J. Vučković, *Phys. Rev. B* **86**, 195312 (2012).
- [45] R. Bose, T. Cai, K. R. Choudhury, G. S. Solomon, and E. Waks, *Nat. Photon.* **8**, 858 (2014).
- [46] T. C. H. Liew and V. Savona, *Phys. Rev. Lett.* **104**, 183601 (2010).
- [47] M. Bamba, A. Imamoğlu, I. Carusotto, and C. Ciuti, *Phys. Rev. A* **83**, 021802(R) (2011).
- [48] Y. Ota, S. Iwamoto, N. Kumagai, and Y. Arakawa, *Phys. Rev. Lett.* **107**, 233602 (2011).
- [49] E. del Valle, S. Zippilli, F. P. Laussy, A. Gonzalez-Tudela, G. Morigi, and C. Tejedor, *Phys. Rev. B* **81**, 035302 (2010).
- [50] K. Kuruma, Y. Ota, M. Kakuda, D. Takamiya, S. Iwamoto, and Y. Arakawa, *Appl. Phys. Lett.* **109**, 071110 (2016).
- [51] R. Trotta, E. Zallo, E. Magerl, O. G. Schmidt, and A. Rastelli, *Phys. Rev. B* **88**, 155312 (2013).
- [52] J. Vučković and Y. Yamamoto, *Appl. Phys. Lett.* **82**, 2374 (2003).
- [53] S. Mosor, J. Hendrickson, B. C. Richards, J. Sweet, G. Khitrova, H. M. Gibbs, T. Yoshie, A. Scherer, O. B. Shchekin, and D. G. Deppe, *Appl. Phys. Lett.* **87**, 141105 (2005).
- [54] R. Konoike, M. Nakadai, Y. Tanaka, T. Asano, and S. Noda, Experimental study of electrical dynamic control of coupling strength between photonic-crystal nanocavities, in The 77th JSAP Autumn Meeting, Niigata, Japan, 2016, 14p-P14-4.
- [55] R. Konoike, H. Nakagawa, M. Nakadai, T. Asano, Y. Tanaka, and S. Noda, *Sci. Adv.* **2**, e1501690 (2016).
- [56] K. M. Birnbaum, A. Boca, R. Miller, A. D. Boozer, T. E. Northup, and H. J. Kimble, *Nature (London)* **436**, 87 (2005).
- [57] S. S. Shamailov, A. S. Parkins, M. J. Collett, and H. J. Carmichael, *Opt. Commun.* **283**, 766 (2010).
- [58] H. J. Carmichael, *Statistical Methods in Quantum Optics I: Master Equations and Fokker-Planck Equations*, 2nd ed. (Springer, Berlin, 2003).
- [59] D. Takamiya, Y. Ota, R. Ohta, H. Takagi, N. Kumagai, S. Ishida, S. Iwamoto, and Y. Arakawa, Large vacuum Rabi splitting in an H0 photonic crystal nanocavity-quantum dot system, in *2013 Conference on Lasers and Electro-Optics Pacific Rim* (Optical Society of America, 2013), paper MI2_2.
- [60] Y. Ota *et al.* (unpublished).
- [61] F. Troiani, J. I. Perea, and C. Tejedor, *Phys. Rev. B* **74**, 235310 (2006).
- [62] M. O. Scully, B. G. Englert, and H. Walther, *Nature (London)* **351**, 111 (1991).
- [63] Y. Tanaka, J. Upham, T. Nagashima, T. Sugiya, T. Asano, and S. Noda, *Nat. Mater.* **6**, 862 (2007).
- [64] K. Kamide, S. Iwamoto, and Y. Arakawa, *Phys. Rev. A* **92**, 033833 (2015).
- [65] J. R. Schrieffer and P. A. Wolff, *Phys. Rev.* **149**, 491 (1966).
- [66] D. F. V. James, P. G. Kwiat, W. J. Munro, and A. G. White, *Phys. Rev. A* **64**, 052312 (2001).
- [67] W. K. Wootters, *Phys. Rev. Lett.* **80**, 2245 (1998).